Molecular cloning, expression, and subcellular localization of a *PAL* gene from *Citrus reticulata* under iron deficiency

H.Y. YANG[1], T. DONG[2], J.F. LI[3], and M.Y. WANG[1]*

Department of Horticulture, Huaqiao University, Xiamen, P.R. China[1]
Institute of Fruit Tree Research, Guangdong Academy of Agricultural Sciences, Guangzhou, P.R. China[2]
School of Agriculture and Biology, Shanghai Jiaotong University, Shanghai, P.R. China[3]

Abstract

Phenylalanine ammonia lyase (PAL) is a specific branch point enzyme of primary and secondary metabolism. The *Citrus reticulata* Blanco *PAL* gene was cloned and designated as *CrPAL1*. The cDNA sequence of *CrPAL1* was 2 166 bp, encoding 721 amino acid residues. Sequence alignment indicates that *CrPAL1* shared a high identity with *PAL* genes found in other plants. Both the dominant and catalytic active sites of *CrPAL1* were similar to PAL proteins observed in *Petroselinum crispum*. Phylogenetic tree analysis indicates that *CrPAL1* was more closely related to *PAL*s in *Citrus clementina* × *C. reticulata* and *Poncirus trifoliata* than to those from other plants. Subcellular localization reveals that CrPAL1-green fluorescent protein fusion protein was specifically localized in the plasma membrane. Activity of PAL as well as *CrPAL1* expression increased under Fe deficiency. A similar result was noted for total phenolic content. The root exudates of *C. reticulata* strongly promoted reutilization of apoplastic Fe in roots. Furthermore, Fe was more desorbed from the cell wall under Fe deficiency than in sufficient Fe supply.

Additional key words: phenolics, phenylalanine ammonia lyase, root exudation.

Introduction

Phenylalanine ammonia lyase (PAL, EC 4.3.1.5) is the first key enzyme of the phenylpropaniod pathway, which produces many important secondary metabolites including flavonoids, plant hormones, anthocyanins, lignins, phytoalexins, and many other important compounds in higher plants (Song and Wang 2009, Vogt 2010, Fraser and Chapple 2011). The PAL mediates a conversion of phenylalanine to cinnamic acid (Mandal *et al*. 2010, Zhang *et al*. 2013). So far, *PAL* genes have been cloned from several plants including *Arabidopsis thaliana* (Cochrane *et al*. 2004), *Pisum sativum*, *Nicotiana tabacum* (Pellegrini *et al*. 1994), rice (Minami *et al*. 1989), and potato (Joos and Hahlbrock 1992).

Citrus reticulata Blanco is an important rootstock in nursery, and iron is essential for its growth and development (Kacar *et al*. 2014). Most citrus plants are cultivated in mountainous areas and are frequently challenged with iron deficiency (Pestana *et al*. 2012, Wulandari *et al*. 2014). The solubility of iron in soil is affected by pH and in soil with high pH, Fe^{2+} is converted into Fe^{3+} and so it is less available. Moreover, a high P content reduces absorption of Fe (Brown 1980). Iron deficiency is a key limiting factor for fruit production and quality (Álvarez-Fernández *et al*. 2011), but *C. reticulata* is partially adapted to Fe deficiency through secretion of phenolic compounds to promote Fe solubilization (Zhang *et al*. 1991, Cesco *et al*. 2010).

Phenolic compounds are important secondary metabolites (Cesco *et al*. 2010) and PAL plays an important role in plant phenolic metabolism. Therefore, we cloned the full-length *PAL* gene, studied the structure of it, and then investigated expression of the *PAL* gene in Fe-deficient roots in parallel with analysis of PAL activity.

Materials and methods

Plants and experimental design: *Citrus reticulata* Blanco seeds from the Huazhong Agricultural University were surface sterilized with 75 % (v/v) ethanol for 10 min, rinsed with sterile double distilled water (ddH$_2$O), placed on moist filter paper, and germinated in an incubator at 26 °C. River sand and *Vermiculite* (3:1, v/v) were cleaned with 1 M hydrochloric acid to remove Fe ions and then autoclaved at 121 °C for 2 h. Three uniform seedlings were transplanted to a 12 cm diameter plastic pot filled with 2.5 kg of the above substrate.

The experiment was a completely randomized design with two Fe treatments (Fe-sufficiency and Fe-deficiency) and each treatment had six replicates. The pots were irrigated twice a week with 200 cm^3 of a half-strength Hoagland's nutrient solution according to Li *et al*. (2015). Iron was added as *o,o*-FeEDDHA in two different concentrations: 50 μM (Fe-sufficient treatment) and 0 μM (Fe-deficient treatment). The nutrient solution pH was 6.0 ± 0.1. The seedlings were cultivated in a greenhouse under night/day temperatures of 16-18/26-28 °C and a natural irradiance and photoperiod. Eight weeks later, roots were harvested, immediately frozen in liquid nitrogen, and stored at -80 °C.

Determination of total phenolics: Phenolics in root exudates from *C. reticulata* Blanco were extracted by the methods of Xu *et al*. (2007). The collected root exudates were evaporated to dryness and the residue was dissolved in methanol (Schieber *et al*. 2001). The total phenolic content was measured using the Folin-Ciocalteu method with absorbance measured at 765 nm using a spectro-photometer (*UV-3600, Shimadzu, Japan*) and compared with a gallic acid standard (Waterman and Mole 1994).

Desorption of Fe bound to the cell wall: The cell wall was extracted according to Zhong and Läuchli (1993) with modifications according to Li *et al*. (2015). The final pellet was freeze-dried overnight and the cell wall powder was stored at 4 °C. The desorption kinetics of the root exudates was analyzed according to Jin *et al*. (2007). Approximately 0.05 g of the cell wall powder was added into a 2 cm^3 column equipped with a filter at the bottom. The solution was run through using a peristaltic pump at a speed of 2 cm^3 per 10 min. It was then collected by a fraction collector at 10 min intervals, and Fe in the desorbed solutions was determined with 2,2-bipyridyl according to Bienfait *et al*. (1985). Finally, cumulative Fe desorbed was calculated and plotted against total desorption volumes.

Isolation of RNA and cDNA synthesis: The total RNA from frozen roots was extracted using an *RNAprep* pure tissue kit (*Tiangen*, Beijing, China). The DNA was removed using an *RNAclean* kit (*Tiangen*). Concentration, purity, and integrity of RNA were determined by spectrophotometric analysis (A$_{260}$/A$_{280}$) and examined by electrophoresis on a 1.0 % (m/v) agarose gel. The first-strand of cDNA was synthesized with a cDNA synthesis kit (*TaKaRa*, Dalian, China). The synthesized cDNA product was diluted appropriately and stored at -20 °C until further analysis.

Cloning *CrPAL1* cDNA: *CrPAL1* cDNA was obtained by reverse transcriptase-polymerase chain reaction. Specific primers (Table 1) were designed by the *Primer Premier 5.0* software based on a multiple sequence alignment of the known *PAL* sequences of *Citrus sinensis*, *Citrus clementina* × *Citrus reticulata*, and other plants in *GenBank*. The primers were synthesized by *Sangon Biotechnology Co*. (Shanghai, China). The PCR reaction was carried out in a final volume of 50 mm^3 containing 5 mm^3 of 10× *Ex Taq* buffer (Mg^{2+} plus), 4 mm^3 of 2.5 mM each dNTP mixture, 2 mm^3 of each primer, 40 ng of template, 0.5 mm^3 of *TaKaRa Ex Taq* (5 U mm^{-3}) and 36.5 mm^3 of ddH$_2$O. Conditions for PCR were: 94 °C for 5 min, 30 cycles (94 °C for 30 s, 55 °C for 30 s, 72 °C for 2.5 min), and 72 °C for 7 min. The PCR products were purified and transformed into *E. coli* strain DH5α competent cells using the *pMD-18T* vector (*TaKaRa*). The transformed cells were inoculated on a solid selection lysogeny broth (LB) medium containing X-Gal, isopropyl-β-d-thiogalactoside (IPTG), and ampicillin. White positive colonies were cultured in liquid LB media for 16 h to extract plasmids, which were purified and sequenced by *Sangon Biotechnology Co*.

Sequence analysis: The vector *NTI Advance$^@$ 11.5* was used to translate an open reading frame (ORF), align sequences, and calculate the molecular mass of the predicted protein. Multiple alignment analysis was performed by *Clustal W. BLAST via NCBI* (http://www. ncbi.nlm.nih.gov/). The website of *Expasy Molecular Biology Server* (http://www.cn.expasy.org/tools/) was used to analyze the structure of the predicted PAL protein. Homology-based structure modelling was done with *Swiss-Model* (Guex and Peitsch 1997). The transcription start site was forecast by the *Neural Network Promoter Prediction* software (http://www. fruitfly.org/seq_tools/promoter.html). *Web Lab View Lite 4.0* was used to display 3-D structures. Phylogenetic analysis was built using the *MEGA 5.1* software by the neighbor-joining method.

Subcellular localization: For generation of *CrPAL1-mGFP5*, the ORF of the *CrPAL1* cDNA was PCR amplified using respective primers (Table 1). The fragment was cloned into *CrPAL1-mGFP5* under control of the CaMV35 promoter of pCAMBIA1302. *Agrobacterium* strain GV3101 carrying the constructs was grown overnight in a Murashige and Skoog solid

medium containing 50 µg cm⁻³ kanamycin and 50 µg cm⁻³ rifampicin. The fusion expression vector (pCAMBIA1302-CrPAL1) was transformed into the inner epidermis of onion (*Allium cepa*). For comparison, pCAMBIA1302 was transiently expressed in the inner epidermis of onion. Green fluorescent protein (GFP) was visualized using an *LSM 5 Exciter* confocal laser scanning microscope (*LSM 710*, *Carl-Zeiss*, Germany) with excitation at 488 nm and emission at 505 to 530 nm (Du *et al.* 2012).

Determination of PAL activity: Fresh roots (100 mg) were ground with 2.0 cm³ of a solution containing 50 mM phosphate buffer (pH 7.0), 1 % (m/v) polyvinylpoly-pyrrolidone, and 0.2 mM ascorbic acid. After centrifugation at 4 000 *g* and 4 °C for 15 min, the supernatant was spectrometrically (*UV-3600*, *Shimadzu*) analyzed for PAL activity at 290 nm using L-phenylalanine (*Sigma-Aldrich*, St. Louis, MO, USA) as substrate (Boo *et al.* 2011).

Expression analysis of *CrPAL1* by real time quantitative PCR (qPCR) was conducted using an *Applied Biosystems 7500* system (Foster City, CA, USA) in roots under Fe-deficiency. Specific primersfor *CrPAL1* and *β-actin* (Table 1) were designed using the *Primer Premier 5.0* software and synthesized by *Sangon Biotechnology Co*. A 25 mm³ of a reaction mixture contained 12.5 mm³ of *MightyAmp* real time (*SYBR Plus*), 0.5 mm³ of a PCR forward primer (10 µM), 0.5 mm³ of a PCR reverse primer (10 µM), 2 mm³ of a template, and 9.5 mm³ of ddH₂O. The PCR program was: the first cycle at 95 °C for 30 s followed by 40 cycles of 5 s at 95 °C, 45 s at 60 °C, and a final extension at 72 °C for 30 s. Melting curve analysis was performed under the following conditions: 10 s at 70 °C and heating to 100 °C at a rate of 0.2 °C s⁻¹. The *actin* gene was chosen as reference under the same conditions. The relative expression of the *PAL* gene was calculated by the $2^{-\Delta\Delta Ct}$ method (Livak and Schmittgen 2001).

Statistical analysis: All data were subjected to one-way *ANOVA* using the *SAS v. 8.0* software (*SAS Institute Inc.*, Cary, USA). Significant differences between treatments were determined by one-way *ANOVA* at $P < 0.05$.

Table 1. Specific primers designed for cloning and real time quantitative PCR amplification.

Gene name	Sequence (5' - 3') - forward	Sequence(5' 3') - reverse	Product size [bp]
PAL	ATGGACAGAGGTGCTGTTATTGAG	CTAGTGCATATTGGAAGAGGGGC	2166
PAL-TF	AGATGTAAACTCCTTGGGACTGA	CGACGGTTAAGACTTTCCTAGCT	188
β-actin	CACACTGGAGTGATGGTTGG	ATTGGCCTTGGGGTTAAGAG	228
ORF	ATGGACAGAGGTGCTGTTATTGAG	GTGCATATTGGAAGAGGGGC	2166

Results

Total phenolic content under the Fe-deficiency was 8.45 µg g⁻¹(root exudates), which was significantly higher
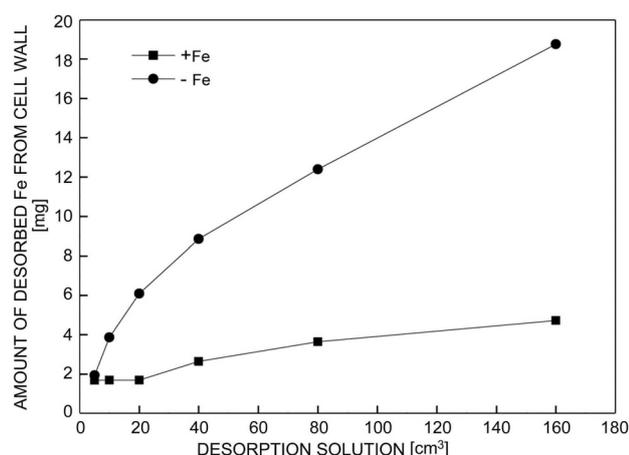

Fig. 1. The desorption kinetic curve of Fe in root cell walls of *Citrus reticulata* under Fe-deficiency (-Fe) and Fe-sufficiency (+Fe).

than in the Fe-sufficient treatment [4.87 µg g⁻¹(root exudates); Table 2]. The content of desorbed Fe increased almost linearly with the volume of the desorption solution (from 40 to 160 cm³; Fig. 1). Only a small amount of apoplastic Fe was desorbed from the cell wall under Fe-sufficiency, and the content of desorbed Fe was obviously higher under the Fe-deficiency than under the Fe-sufficiency.

Based on the known *PAL* sequences of *C. sinensis*, *C. clementina* × *C. reticulata*, and other plants in *GenBank*, the full-length sequence of *PAL1* was obtained by the method of homology cloning from *C. reticulata*. This sequence was named *CrPAL1* (*GenBank* accession No. KP742840). The full-length cDNA of *CrPAL1* was 2 166 bp (Fig. 2). The ORF encoded a protein with 721 amino acids with a predicted molecular mass of 78.6 kDa and a pI of 6.09. *BLAST* analysis reveals that the deduced amino acid sequence of the CrPAL1 protein shared two highly conserved deamination sites and a typical phenylalanine / histidine ammonia lyase protein tag

(Fig. 1 Suppl.). CrPAL1 exhibited a high homology with *Populus trichocarpa* (AFZ78650.1), *Daucus carota* (BAC56977.1), *Vitis vinifera* (AEX32784.1), *Litchi chinensis* (ACR15762.1), *Jatropha curcas* (ABI33979.1), *Ricinus communis* (AGY49231.1), and *Citrus clementina × Citrus reticulata* (CAB42793.1). Furthermore, the results show that CrPAL1 included conserved deamination sites: L213, V214, L261, and A262; and conserved catalytic active sites: N265, G266, NDN (387-389 aa), H401, and HNQDV (491-495 aa) (Fig. 3 Suppl.).

The secondary structure was predicted. The CrPAL1 protein mainly included an alpha helix (48.13 %) and a random coil (28.99 %), whereas an extended strand (13.04 %) and a beta turn (9.85 %) contributed little to the structure (Fig. 4 Suppl.). The predicted three-dimensional structure of the CrPAL1 protein was performed using *Swiss-Model* with the *Petroselinum crispum PAL* protein structure as template (Fig. 3). Average sequence similarities between *CrPAL1* and a *P. crispum PAL* homologue were 83.07 %. The CrPAL1 protein was assumed a 'sea horse' shape.
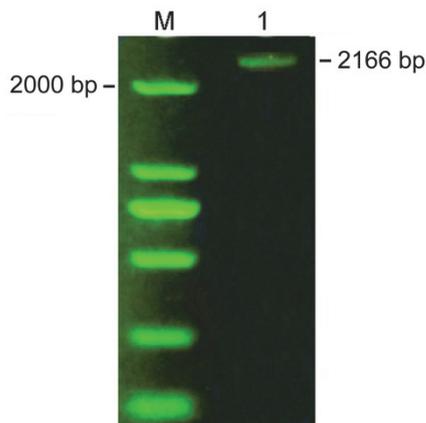

Fig. 2. The full length cDNA of *CrPAL1*. M - 2 kb DNA maker; 1 - *CrPAL1* fragment.

In order to evaluate the structural characteristics of the *PAL* genes in *C. reticulata*, the amino acids were aligned with the PAL proteins from other plants by *MEGA 5.0* analysis. A neighbor-joining phylogenetic tree was divided into three main branches comprising dicotyledons, monocotyledons, and gymnosperms (Fig. 4), which is in accord with a traditional taxonomic classification. The results demonstrate that *CrPAL1* was most close to the *PAL* gene of *P. trifoliata* and *C. clementina × C. reticulata*. Our results also show that *CrPAL1* shared the same ancestor.

Discussion

Citrus is one of the most economically important fruit plants in China. It is cultivated in mountainous areas
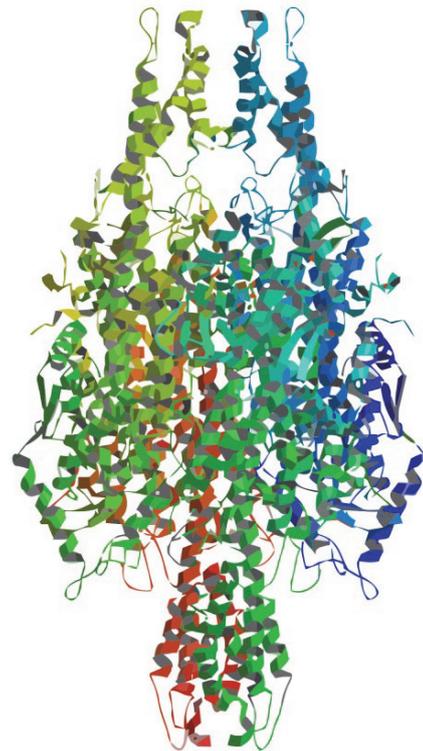

Fig. 3. A schematic illustration of the 3-D structure of the CrPAL1 protein designed using the crystal structure of *Petroselinum crispum* phenylalanine ammonia lyase as template.

The subcellular location of the CrPAL1 protein was analyzed using the GFP as reporter in transient expression assays, and bacterial cells carying *CrPAL1-mGFP5* plasmids were infiltrated into the epidermal cells of onion. Confocal microscopy images demonstrate that the CrPAL1-mGFP5 fusion protein was specifically distributed in the plasma membrane, whereas the GFP alone showed a ubiquitous distribution in the whole cell (Fig. 5). These results suggest that CrPAL1 was a membrane-localized protein.

The PAL activity was analyzed by UV spectro-photometry. The results show that PAL activity was significantly higher (by 16.02 %) under the Fe deficiency than under the Fe sufficiency.

Real time qPCR reveals that expression of the *PAL* gene was affected by the Fe deficiency. Expression of the *PAL1* gene in Fe-deficient roots was significantly higher (1.33 times) than that measured in Fe-sufficient roots (Table 2).

where Fe deficiency is a primary limiting factor for citrus production (Bao *et al.* 2006). *Citrus reticulata* is

important rootstock of citrus cultivars. Thus, research on the *PAL* gene encoding enzyme that is responsible for biosynthesis of phenolics is essential. In this paper, the full-length cDNA of *CrPAL1* was cloned from *Citrus reticulata* using reverse transcriptase PCR. *CrPAL1* encoded a protein with 721 amino acids; its length was similar to that reported for other PALs (Sanchez-Ballesta *et al.* 2000). The sequence alignment shows *CrPAL1* was highly similar to other known *PAL* genes, as to those found in *Poncirus trifoliata*, *C. sinensis*, *C. limon*, *C. clementina* × *C. reticulata*, and *Vitis vinifera* originating from the same branch in the phylogenic tree.

Meanwhile, classical PAL domains and functional sites were found in the deduced PAL protein, such as the conserved deamination sites: L213, V214, L261, and A262; and the conserved catalytic active sites: N265, G266, NDN (387-389 aa), H401, and HNQDV (491-495 aa). These sites are known to be highly conserved in different plants (Song and Wang 2009). In addition, the CrPAL1 protein has a typical protein tag of phenylalanine or histidine ammonia lyase (Ritter and Schulz 2004) suggesting that the deduced amino acid sequence of *CrPAL1* was accurate. All the active sites mentioned above were the same with those of *PAL* mentioned
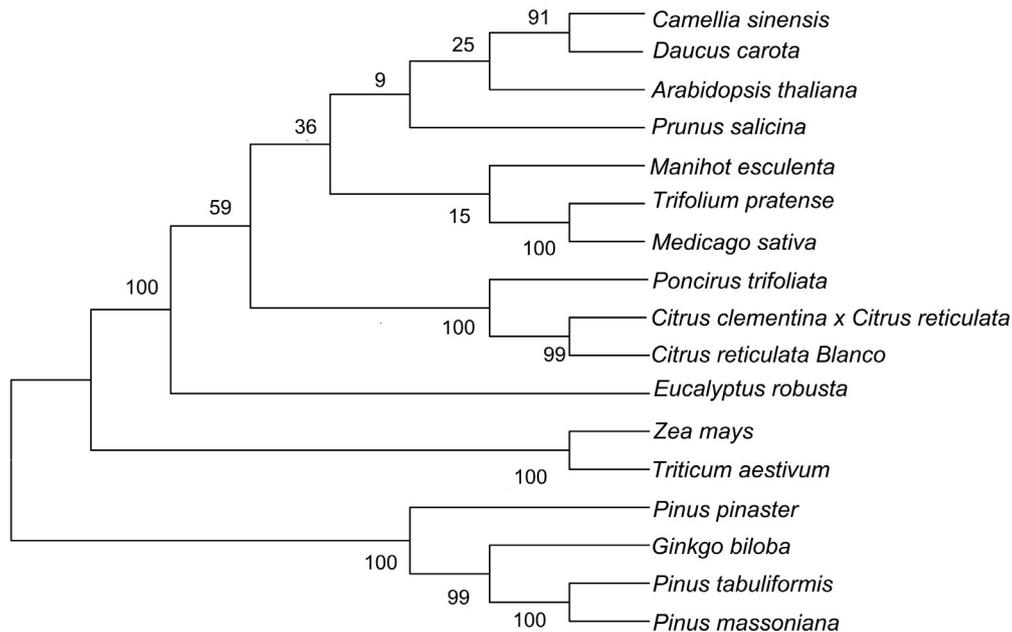

Fig. 4. The phylogenetic analysis of *CrPAL1* with other *PAL* sequences from *Pinus tabuliformis* (AFR79235.1), *P. massoniana* (ACS28225.2), *Ginkgo biloba* (ABU49842.1), *P. pinaster* (CBC83356.1), *Zea mays* (AFW72411.1), *Triticum aestivum* (CAA68036.1), *Citrus clementina* × *Citrus reticulata* (CAB42793.1), *Manihot esculenta* (AAK62030.1), *Prunus salicina* (AFP24940.1), *Camellia sinensis* (P45726.1|), *Daucus carota* (BAG31930.1), *Trifolium pratense* (AAZ29732.1), *Medicago sativa* (CAA41169.1), and *Arabidopsis thaliana* (AAC18870.1).

by Xu *et al.* (2012), indicating that *CrPAL1* is member of the *PAL* gene family.

The subcellular localization of the PAL protein has been studied in different plants (Czichi and Kindl 1975, Hrazdina and Wagner 1985, Rasmussen and Dixon 1999, Achnine *et al.* 2004, Sato *et al.* 2004, Bassard *et al.* 2012). In the present study, the subcellular localization of the CrPAL1 protein was investigated in a heterologous system (the chloroplast-free epidermal cells of onion) by confocal laser-scanning microscopical imaging GFP-fluorescence. A transient expression of the CrPAL1-mGFP5 fusion protein in onion was targeted to the plasma membrane. The result might indicate a high association of the CrPAL1 protein to membranes.

Studies that plant enzymes are involved in phenolic compound syntheses have been associated with plant stress. Phenylalanine ammonia lyase is a well
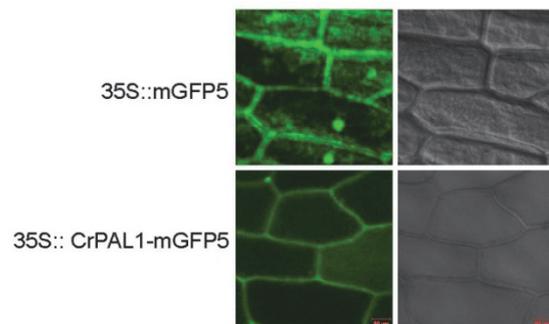

Fig. 5. The subcellular localization of the CrPAL1 protein. Green fluorescent protein fluorescence in onion epidermal cells transfected with a recombinant vector 35S::CrPAL1-mGFP5 and with the empty vector 35S::mGFP5. Time course images were obtained by confocal microscopy after *agro*-infiltration. Dark- and bright-field images are shown.

characterized and key limiting enzyme in the phenylpropanoid pathway (Huang *et al.* 2010). In this experiment, we observed that PAL activity significantly increased under the Fe-deficiency (Table 2). These results are in agreement with recent studies that have shown higher PAL activities in other Fe-deficient plants (Li *et al.* 2015). Consequently, the enhancement of PAL activity promoted accumulation of phenolic compounds to promote Fe solubilization.

Table 2. The impact of iron deficiency on activity of phenylalanine ammonia lyase, relative *CrPAL1* mRNA abundance, and the total phenolic content in *C. reticulata* roots. Means ± SEs of three biological replicates. Statistical significance of differences was determined ($P < 0.05$) by Students *t*-tests and marked with *asterisks*.

	Fe sufficient	Fe deficient
PAL activity [U g^{-1}(f.m.)]	128.50±6.10	149.09±7.50*
Relative mRNA abundance	1.00±0.23	1.33±0.10*
Phenolic content [μg g^{-1}(f.m.)]	4.87±0.29	8.45±0.51*

Furthermore, the Fe deficiency promoted gene expression related to phenolic compound synthesis. Owing to its important role, the *PAL* gene was widely studied in different tissues of plants since its discovery. In this paper, real time qPCR analysis reveals that a high *CrPAL1* expression was found in roots (Table 2). Expression of the *PAL* gene in roots could be induced by different abiotic stimulation, such as low content of nitrogen, phosphate and iron, or by signalling compounds such as methyl jasmonate, jasmonic acid, H_2O_2, and salicylic acid (Hsieh *et al.* 2011). Studies have also discovered that the total amount of phenolic compounds was higher under Fe deficiency (Hell and Stephan 2003). Thus, expression of *CrPAL1* was up-regulated in response to the Fe deficiency, which is consistent with observations of other plants under stress conditions (Wasternack and Parthier 1997). So, this may explain that activation of secondary metabolism is important for successful plant growth under iron stress.

In conclusion, we cloned one *PAL* gene from *Citrus reticulata* Blanco and designated it *CrPAL1*. Regardless of the fact that the functional details of *CrPAL1* are still unclear, its sequence characterization and induced expression in response to a low content of iron suggest that *CrPAL1* might participate in stress response pathways. Thus, *CrPAL1* could be considered as a potential target gene to be used in genetic engineering for creation of transgenic plants with improved stress tolerance.

References

Achnine, L., Blancaflor, E.B., Rasmussen, S., Dixon, R.A.: Colocalization of L-phenylalanine ammonia-lyase and cinnamate 4-hydroxylase for metabolic channeling in phenylpropanoid biosynthesis. - Plant Cell **16**: 3098-3109, 2004.

Álvarez-Fernández, A., Melgar, J.C., Abadia, J., Abadia, A.: Effects of moderate and severe iron deficiency chlorosis on fruit yield, appearance and composition in pear (*Pyrus communis* L.) and peach (*Prunus persica* (L.) Batsch). - Environ. exp. Bot. **71**: 280-286, 2011.

Bao, J.F., Xia, R.X., Peng, S.A., Li, G.H.: Main soil nutrient status of newhall orchards of Hubei province and its effect on fruit quality of newhall orange. - Soils **38**: 75-80, 2006.

Bassard, J.E., Mutterer, J., Duval, F., Werck-Reichhart, D.: A novel method for monitoring the localization of cytochromes P$_{450}$ and other endoplasmic reticulum membrane associated proteins: a tool for investigating the formation of metabolons. - FEBS J. **279**: 1576-1583, 2012.

Bienfait, H.F., Briel, W.V.D., Mesland-Mul, N.T.: Free space iron pools in roots generation and mobilization. - Plant Physiol. **78**: 596-600, 1985.

Boo, H.O., Heo, B.G., Gorinstein, S., Chon, S.U.: Positive effects of temperature and growth conditions on enzymatic and antioxidant status in lettuce plants. - Plant Sci. **181**: 479-484, 2011.

Brown R.: Factors related to iron uptake by dicotyledonous and monocotyledonous plants. ll. The reduction of Fe^{3+} as influenced by roots and inhibitors. - J. Plant Nutr. **2**: 647-660, 1980.

Cesco, S., Neumann, G., Tomasi, N., Pinton, R., Weisskopf, L.: Release of plant-borne flavonoids into the rhizosphere and their role in plant nutrition. - Plant Soil **329**: 1-25, 2010.

Cochrane, F.C., Davin, L.B., Lewis, N.G.: The *Arabidopsis* phenylalanine ammonia lyase gene family: kinetic characterization of the four *PAL* isoforms. - Phytochemistry **65**: 1557-1564, 2004.

Czichi, U., Kindl, H.: Formation of *p*-coumaric acid and *o*-coumaric acid from L-phenylalanine by microsomal membrane fractions from potato: evidence of membrane-bound enzyme complexes. - Planta **125**: 115-125, 1975.

Du, S.C., In, S.H., Byung, K.H.: Requirement of the cytosolic interaction between pathogenesis-related protein10 and leucine-rich repeat protein1 for cell death and defense signaling in pepper. - Plant Cell **24**: 1675-1690, 2012.

Fraser, C.M., Chapple, C.: The phenylpropanoid pathway in *Arabidopsis*. - The Arabidopsis Book. **9**: e0152, 2011.

Guex, N., Peitsch, M.C.: Swiss-Model and the Swiss-Pdb Viewer: an environment for comparative protein modeling. - Electrophoresis **18**: 2714-2723, 1997.

Hell, R., Stephan, U.W.: Iron uptake, trafficking and homeostasis in plants. - Planta **216**: 541-551, 2003.

Hrazdina, G., Wagner, G.J.: Metabolic pathways as enzyme

complexes: evidence for the synthesis of phenylpropanoids and flavonoids on membrane associated enzyme complexes. - Arch. Biochem. Biophys. **237**: 88-100, 1985.

Hsieh, L.S., Hsieh, Y.L., Yeh, C.S., Cheng, C.Y., Yang, C.C., Lee, P.D.: Molecular characterization of a phenylalanine ammonia-lyase gene (*BoPAL1*) from *Bambusa oldhamii*. - Mol. Biol. Rep. **38**: 283-290, 2011.

Huang, J.L., Gu, M., Lai, Z.B., Fan, B.F., Shi, K., Zhou, Y.H., Yu, J.Q., Chen, Z.X.: Functional analysis of the *Arabidopsis PAL* gene family in plant growth, development, and response to environmental stress. - Plant Physiol. **153**: 1526-1538, 2010.

Jin, C.W., You, G.Y., He, Y.F., Tang, C., Wu, P., Zheng, S.J.: Iron deficiency-induced secretion of phenolics facilitates the reutilization of root apoplastic iron in red clover. - Plant Physiol. **144**: 278-285, 2007.

Joos, H.J., Hahlbrock, K.: Phenylalanine ammonia-lyase in potato (*Solanum tuberosum* L.). - Eur. J. Biochem. **204**: 621-629, 1992.

Kacar, Y.A., Simsek, O., Donmez, D., Boncuk, M., Yesiloglu, T., Ollitrault, P.: Genetic relationships of some *Citrus* genotypes based on the candidate iron chlorosis genes. - Turk. J. Agr. Forest. **38**: 340-347, 2014.

Li, J.F., Zheng, W.J., Zeng, L., Liu, J.F., Wang, M.Y.: Molecular cloning, expression and sequence analysis of a phenylalanine ammonia-lyase gene from *Poncirus trifoliata* under iron deficiency. - Aust. J. Bot. **62**: 698-704, 2015.

Livak, K.J., Schmittgen, T.D.: Analysis of relative gene expression data using real-time quantitative PCR and the $2^{-\Delta\Delta CT}$ method. - Methods **25**: 402-408, 2001.

Mandal, S.M., Chakraborty, D., Dey, S.: Phenolic acids act as signaling molecules in plant-microbe symbioses. - Plant Signal. Behav. **5**: 359-368, 2010.

Minami, E.I., Ozeki, Y., Matsuoka, M., Koizuka, N., Tanaka, Y.: Structure and some characterization of the gene for phenylalanine ammonia-lyase from rice plants. - Eur. J. Biochem. **185**: 19-25, 1989.

Pellegrini, L., Rohfritsch, O., Fritig, B., Legrand, M.: Phenylalanine ammonia-lyase in tobacco – molecular cloning and gene expression during the hypersensitive reaction to tobacco mosaic virus and the response to a fungal elicitor. - Plant Physiol. **106**: 877-886, 1994.

Pestana, M., Gama, F., Saavedra, T., De Varennes, A., Correia, P.J.: The root ferric-chelate reductase of *Ceratonia siliqua* (L.) and *Poncirus trifoliata* (L.) Raf. responds differently to a low level of iron. - Sci. Hort. **135**: 65-67, 2012.

Rasmussen, S., Dixon, R.A.: Transgene-mediated and elicitor-induced perturbation of metabolic channeling at the entry point into the phenylpropanoid pathway. - Plant Cell **11**: 1537-1551, 1999.

Ritter, H., Schulz, G.E.: Structural basis for the entrance into the phenylpropanoid metabolism catalyzed by phenylalanine ammonia-lyase. - Plant Cell **16**: 3426-3436, 2004.

Sanchez-Ballesta, M.T., Lafuente, M.T., Zacarias, L., Granell, A.: Involvement of phenylalanine ammonia-lyase in the response of Fortune mandarin fruits to cold temperature. - Physiol Plant. **108**: 382-389, 2000.

Sato, T., Takabe, K., Fujita, M.: Immunolocalization of phenylalanine ammonia-lyase and cinnamate-4-hydroxylase in differentiating xylem of poplar. - Compt. rend. Biol. **327**: 827-836, 2004.

Schieber, A., Keller, P., Carle, R.: Determination of phenolic acids and flavonoids of apple and pear by high-performance liquid chromatography. - J. Chromatogr. A **910**: 265-273, 2001.

Song, J., Wang, Z.: Molecular cloning, expression and characterization of a phenylalanine ammonia-lyase gene (*SmPAL1*) from *Salvia miltiorrhiza*. - Mol. Biol. Rep. **36**: 939-952, 2009.

Vogt, T.: Phenylpropanoid biosynthesis. - Mol. Plants **3**: 2-20, 2010.

Wasternack, C., Parthier, B.: Jasmonate-signalled plant gene expression. - Trends Plant Sci. **2**: 302-307, 1997.

Waterman, P.G., Mole, S.: Analysis of Phenolic Plant Metabolites. - Blackwell Scientific, Oxford - London 1994.

Wulandari, C., Muraki, S., Hisamura, A., Ono, H., Honda, K., Kashima, T., Subandiyah, S.: Effect of iron deficiency on root ferric chelate reductase, proton extursion, biomass production and mineral absorption of citrus root stock orange jasmine (*Murraya exotica* L.). - J. Plant Nutr. **37**: 50-64, 2014.

Xu, F., Deng, G., Cheng, S.Y., Zhang, W.W., Huang, X.H., Li, L.L., Cheng, H., Rong, X.F., Li, J.B.: Molecular cloning, characterization and expression of the phenylalanine ammonia-lyase gene from *Juglans regia*. - Molecules **17**: 7810-7823, 2012.

Xu, W.H., Liu, H., Ma, Q.F., Xiong, Z.T.: Root exudates, rhizosphere Zn fractions, and Zn accumulation of ryegrass at different soil Zn levels. - Pedosphere **17**: 389-396, 2007.

Zhang, F.S., Römheld, V., Marschner, H.: Role of the root apoplasm for iron acquisition by wheat plants. - Plant Physiol. **97**: 1302-1305, 1991.

Zhang, R.Q., Zhu, H.H., Zhao, H.Q., Yao, Q.: Arbuscular mycorrhizal fungal inoculation increases phenolic synthesis in clover roots via hydrogen peroxide, salicylic acid and nitric oxide signaling pathways. - J. Plant Physiol. **170**: 74-79, 2013.

Zhong, H., Läuchli, A.: Changes of cell wall composition and polymer size in primary roots of cotton seedlings under high salinity. - J. exp. Bot. **44**: 773-778, 1993.